Measurement of the 2H(n,γ)3H reaction cross section between 10 and 550 keV

Measurement of the ^{2}H$(n, \gamma)^3$H reaction cross section between 10 and 550 keV

Y. Nagai,[1,*] T. Kobayashi,[2] T. Shima,[1] T. Kikuchi,[2] K. Takaoka,[2] M. Igashira,[3] J. Golak,[4] R. Skibiński,[4] H. Witała,[4] A. Nogga,[5] W. Glöckle,[6] and H. Kamada[7]

[1]*Research Center for Nuclear Physics, Osaka University, Mihogaoka, Ibaraki, Osaka 567-0047, Japan*
[2]*Department of Applied Physics, Tokyo Institute of Technology, O-okayama, Meguro, Tokyo 152-8551, Japan*
[3]*Research Laboratory for Nuclear Reactors, Tokyo Institute of Technology, O-okayama, Meguro, Tokyo 152-8550, Japan*
[4]*M. Smoluchowski Institute of Physics, Jagiellonian University, Krakow 30-059, Poland*
[5]*Institut für Kernphysik (Theorie), Forschungszentrum Jülich, D-52425 Jülich, Germany*
[6]*Institut für Theoretische Physik II, Ruhr-Universität at Bochum, D-44780 Bochum, Germany*
[7]*Department of Physics, Faculty of Engineering, Kyushu Institute of Technology, 1-1 Sensuicho, Tobata, Kitakyushu 804-8550, Japan*

(Received 24 February 2006; published 14 August 2006)

We have measured for the first time the cross section of the ^{2}H$(n, \gamma)^3$H reaction at an energy relevant to big-bang nucleosynthesis by employing a prompt discrete γ-ray detection method. The outgoing photons have been detected by means of anti-Compton NaI(Tl) spectrometers with a large signal-to-noise ratio. The resulting cross sections are 2.23 ± 0.34, 1.99 ± 0.25, and $3.76 \pm 0.41 \mu$b at $E_n = 30.5$, 54.2, and 531 keV, respectively. At $E_n = 30.5$ keV the cross section differs from the value reported previously by a factor of 2. Based on the present data the reaction rate has been obtained for temperatures in the range $10^7 - 10^{10}$ K. The astrophysical impact of the present result is discussed. The obtained cross sections are compared with a theoretical calculation based on the Faddeev approach, which includes meson exchange currents as well as a three-nucleon force.

DOI: 10.1103/PhysRevC.74.025804 PACS number(s): 25.10.+s, 25.40.Lw, 26.60.+c, 26.35.+c

I. INTRODUCTION

The nucleon-capture reaction by the deuterium at astrophysicaly relevant energy plays an important role in nuclear astrophysics. The ^{2}H$(p, \gamma)^3$He reaction was one of the principal methods of ^{4}He production during the primordial nucleosynthesis era [1], and a key reaction during the proto-stars era, in which the energy generated by this deuterium burning would have slowed down the contraction due to the gravitational force [2,3]. Hence, the cross section of the ^{2}H$(p, \gamma)^3$He reaction is important in estimating the abundance of light elements during primordial nucleosynthesis and also in constructing models of proto-stars. However, the ^{2}H$(n, \gamma)^3$H reaction has been claimed to be important in nonstandard inhomogeneous big-bang models [4]. These models, proposed as alternatives to the standard ones, are characterized by both neutron-rich and neutron-poor regions due to a possible first-order phase transition from a quark-dominated to a hadron-dominated universe [5]. In the neutron-rich region, a sufficient amount of intermediate-heavy nuclei would have been produced mainly through a neutron-capture reaction, such as ^{2}H$(n, \gamma)^3$H$(d, n)^4$He$(^3$H, $\gamma)^7$Li$(n, \gamma)^8$Li$(\alpha, n)^{11}$B$(n, \gamma)^{12}$B, etc. [4]. The production yield depends on the cross section, $\sigma_{^2\mathrm{H}}(n, \gamma)$, of the ^{2}H$(n, \gamma)^3$H reaction as well as on the other cross sections mentioned.

The study of the ^{2}H$(n, \gamma)^3$H reaction is interesting from an astrophysical point of view, and the reaction mechanism itself is worth investigating. The measured cross section, $\sigma_{^2\mathrm{H}}(n, \gamma)$, is 0.508 ± 0.015 mb for thermal neutrons [6] and is much smaller than that of the ^{1}H$(n, \gamma)^2$H reaction, 334.2 ± 0.5 mb, for thermal ones [7]. The smallness of the neutron-capture cross section is attributed to the structures of the three-nucleon scattering and bound states [8]. Namely the magnetic dipole ($M1$) transition is not allowed in an impulse approximation between the spin singlet scattering state and the ground state ($1/2^+$) of ^{3}H. Hence, the $M1$ transition must proceed through small components of the wave functions for these states [9]. Therefore, one can expect a large contribution from meson exchange currents to the measured cross section. Actually, the calculated value with the single nucleon current supplemented by two- and three-body currents is 0.556 mb, and the value based on one-body current approximation is 0.227 mb, less than half of the measured one [10]. The origin of the discrepancy of about 10% remains an open problem to be clarified. Hence, it is worthwhile to measure the cross section, $\sigma_{^2\mathrm{H}}(n, \gamma)$, at higher neutron energy to obtain additional information that would lead to better theoretical models for the nucleon-nucleon interaction, the nuclear wave function of ^{3}H and the meson exchange currents.

Experimentally, $\sigma_{^2\mathrm{H}}(n, \gamma)$ has been measured only for thermal neutrons, and therefore the cross section at the stellar energy has been evaluated assuming the charge symmetry while using the measured cross section of the ^{2}H$(p, \gamma)^3$He reaction [11]. The cross section for the ^{2}H$(p, \gamma)^3$He reaction [3,12] and the polarization observables for the ^{1}H$(d, \gamma)^3$He reaction [13] have been measured using polarized p and d beams at the stellar energy; the total ^{2}H$(p, \gamma)^3$He S factor at $E = 0$ was claimed to be smaller by about 37% than the previously reported one [14]. Because of the discrepancy of the ^{1}H$(d, \gamma)^3$He reaction cross section, the ^{2}H$(n, \gamma)^3$H reaction rate is now uncertain. In addition it should be mentioned that in

*Electronic address: nagai@rcnp.osaka-u.ac.jp

a recent study of the ^{1}H$(d,\gamma)^3$He reaction a significant effort was made to measure its cross section at a very low proton lab energy of $E_{^1\mathrm{H(lab.)}} = 4.04$ keV [3]. The enhancement of the S factor due to electron screening effects is expected to be as large as 6% at the center-of-mass energy of $E_{\mathrm{c.m.}} = 2.5$ keV and 20% at $E_{\mathrm{c.m.}} \simeq 1$ keV, but its magnitude is hard to verify experimentally using the current technique [3]. Because charge symmetry holds well in the relevant nuclear reaction, it is instructive to use the ^{2}H$(n,\gamma)^3$H reaction by measuring $\sigma_{^2\mathrm{H}}(n,\gamma)$ at the stellar energy to study the screening effect.

For these nuclear physics and astrophysical reasons we aimed at measuring $\sigma_{^2\mathrm{H}}(n,\gamma)$ accurately in the keV region.

II. EXPERIMENTAL PROCEDURE

In measuring $\sigma_{^2\mathrm{H}}(n,\gamma)$ in the keV region the following issues have to be considered. First, the cross section obtained by extrapolation using the measured thermal capture cross section of 0.5 mb, and assuming the $1/v$ law is very small, on the order of 1 μb at $E_n \sim 30$ keV. Hence, a γ-ray spectrometer to detect the photon from the ^{2}H$(n,\gamma)^3$H reaction must be well shielded against scattered neutrons from a sample and the γ-ray background. Note that although $\sigma_{^2\mathrm{H}}(n,\gamma)$ is very small at the keV region, the elastic-scattering cross section on the deuterium is quite large, ~3.3 b [15], what is more than 10^6 times larger. It follows that a considerable number of the neutrons reaching the deuterium sample would be scattered and enter a γ-ray detector, if they were not eliminated before entering. The neutrons scattered by the sample and/or various materials in the measuring room would be captured by various materials, such as iron (with a large neutron capture cross section) placed near to a γ-ray spectrometer and produce a large γ-ray background. Second, the γ-ray energy from the ^{2}H(n,γ) reaction is as high as ~6.26 MeV, and therefore a γ-ray detector should have a high detection efficiency for the relevant energies. Third, we must use a deuterium sample not containing any heavy elements with the large neutron capture cross section to measure the γ-ray spectrum of the ^{2}H$(n,\gamma)^3$H reaction with a high signal-to-noise ratio. Finally, the deuterium sample should be free from any hydrogen contaminant to make the correction factor of multiple scattering effects of the incident neutrons in the deuteron sample small, and thereby to determine $\sigma_{^2\mathrm{H}}(n,\gamma)$ accurately, as described later.

To meet the requirements mentioned above, we employed a discrete γ-ray detection method with the use of highly sensitive anti-Compton NaI(Tl) spectrometers, which enabled us to pick up a small signal necessary to unambiguously identify the final ^{3}H nucleus with a good signal-to-noise ratio, shown below.

Pulsed keV neutrons were produced by the ^{7}Li$(p,n)^7$Be reaction. Bunched proton beams of 1.5 ns width were provided from the 3.2 MV Pelletron Accelerator of the Research Laboratory for Nuclear Reactors at the Tokyo Institute of Technology, and the proton energies were adjusted so as to produce neutrons with energy between 10 and 80 keV or with an average energy of 531 keV.

A. Measurement at 10 < E_n < 80 keV

The measurement was performed with an averaged proton beam current of about 5.6μA at a repetition rate of 2 MHz. The neutron energy spectrum from the ^{7}Li$(p,n)^7$Be reaction was measured with a time-of-flight (TOF) technique by a ^{6}Li-glass scintillation detector. The detector was set 34 cm away from the Li target at an angle of 14° with respect to the proton beam direction. Thus, the averaged energy spectrum was obtained on a sample because of the reaction kinematics. We used two samples: ^2H_2O (99.99% enriched in ^{2}H) with a diameter of 90 mm and a thickness of 20 mm and Au with the same diameter and a thickness of 1 mm. The Au sample was used for normalization of the absolute cross section, because the capture cross section is known with good accuracy [16]. The ^2H_2O sample was contained in the acrylic container with an internal diameter of 90 mm and a thickness of 0.5 mm. The thickness of the ^2H_2O sample and the container was determined to minimize any correction factors due to neutron multiple-scattering effects and neutron shielding in the sample and in the container. The samples were placed 12 cm away from the neutron target at an angle of 0° with respect to the proton beam direction. The experiment was carried out by repeating three runs on ^2H_2O, Au, and blank samples cyclically to minimize the effects of any possible changes of the experimental conditions, such as the proton energy and the neutron yield due to a deterioration of the Li target, etc. These runs were associated with the neutron counts registered by the ^{6}Li glass scintillation detector.

The prompt γ ray from the neutron capture by ^{2}H to the ground state in ^{3}H was detected by four NaI(Tl) spectrometers [17]. The spectrometer consisted of a central NaI(Tl) detector with a diameter of 229 mm and a length of 203 mm, and of a plastic annular counter with a thickness of 51 mm for rejecting cosmic muons [17]. The TOF spectra were taken to determine the neutron energy by using the signals from the central NaI(Tl) detectors and the pulsed protons, which were detected by a capacitive time pickoff. The data of the pulse height and the TOF spectrum were stored on a hard disk drive in a list mode. The spectrometers were shielded with ^{6}LiH, B-doped paraffin, and Cd against the neutrons mentioned above. The lead shields were also used to attenuate external γ rays from natural radioactivity and the thermal-neutron capture reactions on various materials. The distance between the front head of the γ-ray spectrometers and the sample position was 60 cm. These spectrometers were set at 125° with respect to the proton beam direction, where the second Legendre polynomial is zero, and thus the γ-ray intensity measured at this angle gives an angle-integrated one for a dipole transition. Further experimental details can be found in [17].

B. Measurement at E_n = 531 keV

The proton energy was adjusted at 2.26 MeV to produce 531 keV neutrons, and the neutron energy spectrum measured by a ^{6}Li glass detector is shown in Fig. 1. Note that the proton energy was well below the threshold energy to populate the first excited state at $E_{\mathrm{ex}} = 429$ keV in ^{7}Be, and therefore we see only quasimonoenergetic neutrons, as shown in Fig. 1. The averaged proton beam current was about 12.2 μA at a

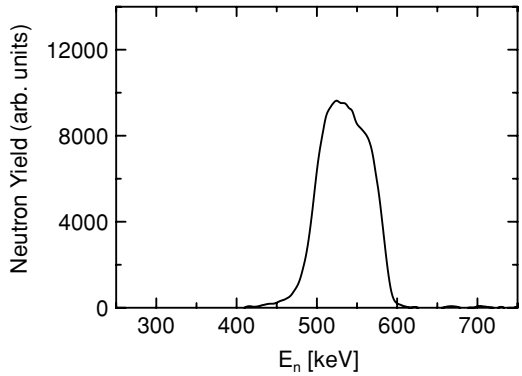

FIG. 1. Neutron energy spectrum taken by a ^{6}Li glass scintillation detector with a TOF method.

repetition rate of 4 MHz. The ^{6}Li glass detector was set 4.5 m away from the Li target at an angle of 9.6° with respect to the proton beam direction. An enriched (99.99%) ^2H_2O sample with a diameter of 90 mm and a thickness of 30 mm was used to obtain a sufficient γ-ray yield from the ^{2}H$(n, \gamma)^3$H reaction. Two samples of ^2H_2O and Au were placed 20 cm away from the neutron target. The prompt γ ray from the reaction was detected by an anti-Compton NaI(Tl) spectrometer [18]. The spectrometer was composed of a central NaI(Tl) detector with a diameter of 152 mm and a length of 203 mm, and an annular one with a diameter of 330 mm and a length of 356 mm [18]. At this point the sensitivity of the spectrometer should be described. When the incident neutron energy is low below 80 keV, the neutrons are emitted from the Li target within a narrow cone with respect to the proton beam direction. Hence, they do not hit the spectrometer directly and thus the above-mentioned shield is good enough to attenuate the events due to the scattered neutrons. However, when the neutron energy is as high as ~500 keV, the neutrons are emitted from the Li target position in a larger cone with respect to the proton beam direction compared to the cone for the low-energy keV neutrons [19]. Consequently, the high-energy neutrons can be directly captured by ^{127}I in the NaI(Tl) spectrometer, producing a $(6.8 + E_{\text{c.m.}})$ MeV γ-ray background from the ^{127}I$(n, \gamma)^{128}$I reaction, just above the 6.63 MeV γ-ray line from the 530 keV neutron capture by ^{2}H. Here, $E_{\text{c.m.}}$ is the center-of-mass energy. Therefore, we made special efforts to reduce the background by using shield materials (Pb and borated paraffin) surrounding ^{6}LiH with different shapes and compositions [20]. The distance between the spectrometer and the sample position was 80 cm.

III. EXPERIMENTAL RESULTS AND DISCUSSIONS

The TOF spectrum was measured by the central NaI(Tl) detector(s) to obtain the background-free (net) γ-ray yields from the ^{2}H$(n, \gamma)^3$H reaction as a function of the neutron energy. A typical TOF spectrum measured for Au at $E_n =$ 531 keV is shown in Fig. 2. Here, the sharp peak at around 0 ns is due to the high-energy γ-rays from the ^{7}Li$(p, \gamma)^8$Be reaction at the neutron production target position, and the broad one at around 40 ns is due to the keV neutron capture

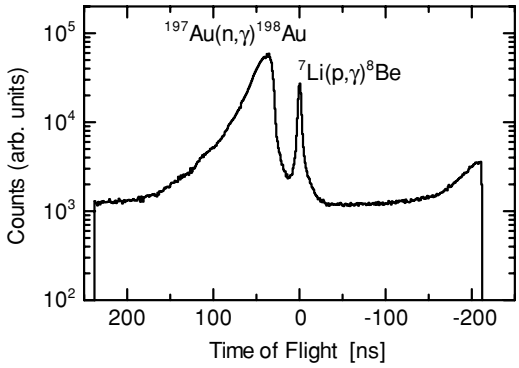

FIG. 2. TOF spectrum for ^{197}Au taken by the NaI(Tl) detector at $E_n = 531$ keV. The peak at 0 ns is from the ^{7}Li$(p, \gamma)^8$Be reaction and the broad peak is due to the γ ray from the keV neutron capture reaction by ^{197}Au.

reaction of Au. The foreground (FG) including background, and background (BG) γ-ray spectra from the ^{2}H$(n, \gamma)^3$H reaction were obtained by putting gates in the proper regions on the TOF spectrum.

A. ^{2}H$(n, \gamma)^3$H reaction at $10 < E_n < 80$ keV

The foreground, background, and net spectra for the neutron energy range from 20 to 40 keV are shown in Fig. 3. In the

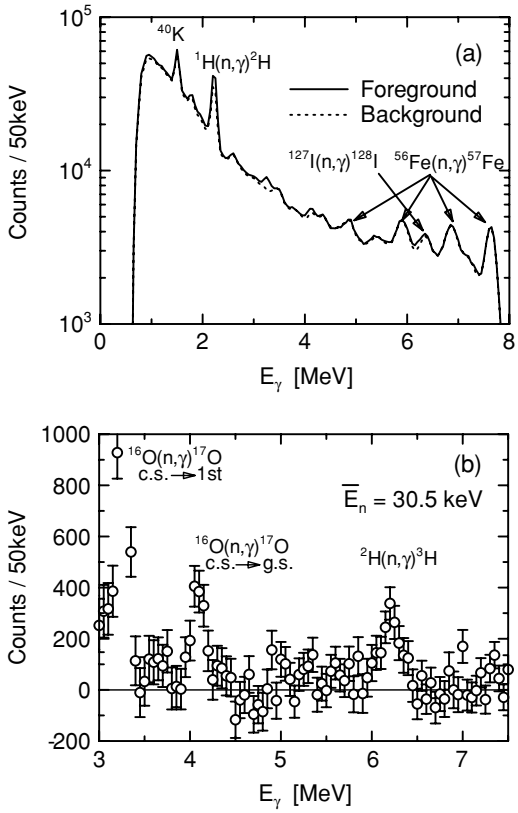

FIG. 3. γ-ray pulse height spectra from the ^{2}H$(n, \gamma)^3$H reaction. (a) Foreground and background spectra are respectively shown as the solid and dotted lines at $10 < E_n < 80$ keV. (b) Background subtracted spectrum at $20 < E_n < 40$ keV is shown.

background spectrum, one sees several γ rays from thermal-neutron capture reactions on ^{1}H and ^{56}Fe in addition to the 1.46 MeV γ ray from the decay of ^{40}K. Here, ^{1}H was contained in an acrylic container and a ^{6}LiH neutron shield placed in front of the central NaI(Tl) detectors, and ^{56}Fe was used as a beam duct and also to support the NaI(Tl) spectrometers. In the net spectrum we observed for the first time the 6.28 MeV γ ray due to a direct neutron capture by deuterium into the ground state in ^{3}H being free from the background γ-rays from the (n, γ) reaction on ^{56}Fe. Three other observed peaks of 2.22, 3.30, and 4.17 MeV are due to the ^{1}H$(n, \gamma)^{2}$H reaction in the acrylic container (2.22 MeV), and direct neutron capture by ^{16}O into the first excited $(1/2^{+})$ 3.30 MeV and ground $(5/2^{+})$ states (4.17 MeV) in ^{17}O, respectively [21]. The γ-ray detector was calibrated using standard sources, such as ^{22}Na, ^{60}Co, and ^{137}Cs, the background γ-ray peaks of 1.461 MeV (^{40}K) and 2.615 MeV (^{208}Tl), and the γ rays from the ^{56}Fe$(n, \gamma)^{57}$Fe reaction, respectively.

B. ^{2}H$(n, \gamma)^{3}$H reaction at $E_n = 531$ keV

Following a similar process described above, the background-subtracted γ-ray spectrum for the $^{2}H_2O$ sample was obtained as shown in Fig. 4. Here, we can clearly see the 6.61 MeV γ ray from the direct capture of 531 keV neutrons by ^{2}H into the ground state in ^{3}H and that three other peaks at 2.49, 3.77, and 4.64 MeV are due to the γ rays from the (n, γ) reaction by ^{1}H (2.49 MeV) and ^{16}O (3.77 and 4.64 MeV), respectively.

C. Cross section of the ^{2}H$(n, \gamma)^{3}$H reaction

To obtain $\sigma_{^2\mathrm{H}}(n, \gamma)$, the γ-ray peak intensities in the net spectrum mentioned above were analyzed by a stripping method by using the response function of the NaI(Tl) spectrometers [17,18]. The cross section, $\sigma_{^2\mathrm{H}}(n, \gamma)$, is given as

$$\sigma_{^2\mathrm{H}}(n, \gamma) = C \times \frac{(\phi)_{\mathrm{Au}}}{(\phi)_{^2\mathrm{H}}} \times \frac{(r^2 n)_{\mathrm{Au}}}{(r^2 n)_{^2\mathrm{H}}} \times \frac{Y_\gamma(^2\mathrm{H})}{Y_\gamma(\mathrm{Au})} \times \sigma_{\mathrm{Au}}(n, \gamma). \quad (1)$$

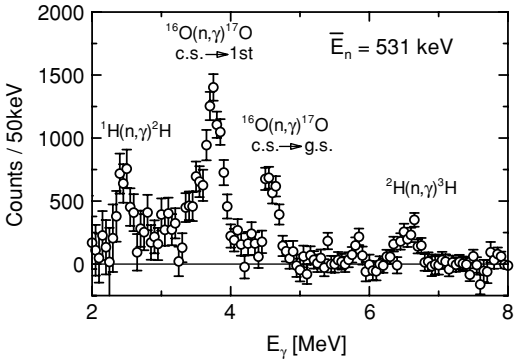

FIG. 4. Background subtracted spectrum from the ^{2}H$(n, \gamma)^{3}$H reaction at $E_n = 531$ keV.

TABLE I. Correction factors used in the analysis for Au and C samples at the averaged neutron energies of 30.5, 54.2, and 531 keV, respectively.

Sample	E_n (keV)	C_{nm}	C_{ns}	$C_{\mathrm{nm}} \times C_{\mathrm{ns}}$
Au	30.5	1.146	0.962	1.103
	54.2	1.121	0.966	1.084
	531	1.075	0.982	1.056
C	30.5	1.835	0.717	1.316
	54.2	1.386	0.727	1.007
	531	1.531	0.631	0.966

Here, C is given by

$$C = \frac{(C_{\mathrm{nm}} C_{\mathrm{ns}} C_{\gamma\mathrm{a}} C_{\gamma\mathrm{g}})_{\mathrm{Au}}}{(C_{\mathrm{nm}} C_{\mathrm{ns}} C_{\gamma\mathrm{a}} C_{\gamma\mathrm{g}})_{^2\mathrm{H}}}. \quad (2)$$

In Eq. (1), $(\phi)_{\mathrm{Au}}$, $Y_\gamma(\mathrm{Au})$, r, and n are the yield of the neutron, the yield of the γ ray, the radius, and the thickness (atomsperbarn) of the Au sample, respectively. $\sigma_{\mathrm{Au}}(n, \gamma)$ is the absolute capture cross section of Au. The correction factor, C, comprises four factors (C_{nm}, C_{ns}, $C_{\gamma\mathrm{a}}$, and $C_{\gamma\mathrm{g}}$), as defined in Eq. (2). The C_{nm} and C_{ns} factors are introduced to correct for multiple scattering and the shielding of the incident neutrons in the sample, respectively. They were calculated using the Monte Carlo code, TIME-MULTI [22]. The $C_{\gamma\mathrm{a}}$ and $C_{\gamma\mathrm{g}}$ factors account for the γ-ray absorption by the sample, and the finite size of the sample, respectively, and they were calculated using a Monte Carlo method [17]. The correction factors obtained in this way are given for the $^{2}H_2O$ and Au samples in Table I.

Finally, the cross section $\sigma_{^2\mathrm{H}}(n, \gamma)$ was obtained for the first time as being 2.23 ± 0.34, 1.99 ± 0.25, and 3.76 ± 0.41 μb at 30.5, 54.2, and 531 keV, respectively. Here, the quoted uncertainty is the result of the combined uncertainties of the γ-ray yield statistics (~2–8%), the response function of the NaI(Tl) spectrometer (2%), the absolute cross section of Au (3%), and the correction factor (3%), respectively. Combining the present results with the measured cross section of $508 \pm 15\mu$b for thermal neutrons [6], the cross section $\sigma_{^2\mathrm{H}}(n, \gamma : E_n)$ can be parametrized as

$$\sigma_{^2\mathrm{H}}(n, \gamma : E_n) = 5.65 \times E_n^{-0.425} + 0.145 \times E_n^{0.5}. \quad (3)$$

Here, we assumed that $\sigma_{^2\mathrm{H}}(n, \gamma : E_n)$ is dominated by the p-wave neutron capture by deuterium as the neutron energy increases in the present energy range. Note that $\sigma_{^2\mathrm{H}}(n, \gamma : E_n)$ and the incident neutron energy E_n are in units of μb and keV in the laboratory system, respectively. The present results are compared to values reported previously [23] in Fig. 5 together with the calculated values discussed below. Note that the previous value was derived by extrapolating the measured thermal-neutron capture cross section by deuterium assuming a $1/v$ law and the measurement on the inverse reaction [23]. The new cross section, $\sigma_{^2\mathrm{H}}(n, \gamma : E_n)$ is significantly different from the previous value; $\sigma_{^2\mathrm{H}}(n, \gamma : E_n)$ at $E_n =$ 30 keV is about two times larger. In Table II and Fig. 5 we compare the experimental results with a present theory.

The theoretical predictions are based on the Faddeev scheme [24] in momentum space. The nuclear matrix element for the neutron-deuteron capture is obtained using time reversal

TABLE II. Measured and calculated cross sections at the averaged neutron energies of 30.5, 54.2, and 531 keV, respectively.

E_n (keV)	$\sigma_{^2\mathrm{H}}(n,\gamma)$ (μb) (exp.)	SNC+ MEC(AV18)	SNC+MEC(AV18)+ Urbana-IX
30.5	2.23±0.34	1.62	1.77
54.2	1.99±0.25	2.30	2.32
531	3.76±0.41	4.16	3.53

from the two-body photodisintegration amplitude, N_μ^{Nd}. The latter is given via the nucleon-deuteron plane wave, $\langle\varphi_1|$, the ^{3}H wave function $|\Psi_b\rangle$, the permutation operator, P, the nuclear electromagnetic current operator, j_μ, and the auxiliary state, $|U\rangle$:

$$N_\mu^{\mathrm{Nd}} = \langle\phi_1|(1+P)|j_\mu|\Psi_b\rangle + \langle\phi_1|P|U\rangle. \quad (4)$$

This state $|U\rangle$ fulfills the Faddeev-like equation:

$$|U\rangle = \big(tG_0 + 0.5(1+P)V_4^{(1)}G_0(tG_0+1)\big)(1+P)j_\mu|\Psi_b\rangle + (tG_0P + 0.5(1+P)V_4^{(1)}G_0(tG_0+1)P)|U\rangle, \quad (5)$$

where t is the t-matrix operator acting on particles 2 and 3, G_0 is the free propagator of three nucleons, and $V_4^{(l)}$ is a part of a three-nucleon force symmetrical under exchanges of nucleons 2 and 3. In the present study the electromagnetic current operator was taken as a sum of the single-nucleon current (SNC) and π- and ρ-like two-body currents (MEC) [25]. As the nuclear interaction, the AV18 potential [26] alone or combined with the Urbana IX three-nucleon force [27] was used. At two lower energies the theoretical results with (without) the three-nucleon force miss the data by about 20(27)% at $E_n = 30.5$ keV and 17(16)% at $E_n = 54.2$ keV. At $E_n = 531$ keV both predictions with and without the three-nucleon force are in agreement with the data (in the range of experimental errors). Here, the difference reaches 6(11)%. At these energies the three-nucleon force effects are small and come mainly from the bound-state wave-function properties. The remaining differences between theoretical and experimental values, at least partially originate in the form of the nuclear current operator used in the calculations. It seems worthwhile to include in the future also other possible exchange currents, neglected in our present framework. The current result is also a challenge to theoreticians to analyze the process under consideration with consistent nuclear potential and currents based on the chiral perturbation theory. Due to small energies it will be an excellent test for this effective approach.

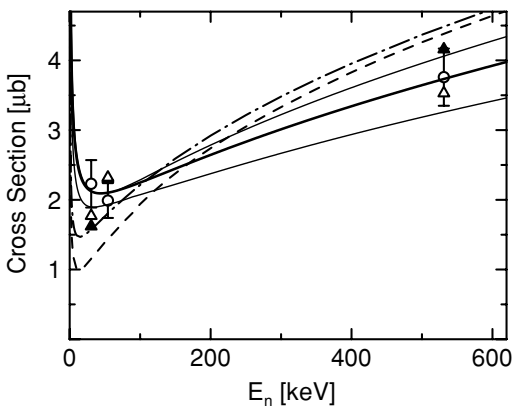

FIG. 5. ^{2}H$(n,\gamma)^3$H cross section vs. neutron energy in the laboratory system. The open circles denote the present results, whereas other symbols indicate the calculated values with single-nucleon current and meson-exchange current (closed triangles), and calculated values with single-nucleon current, meson-exchange current and three-nucleon force (open triangles). The solid curve denotes the most probable cross section curve obtained by fitting the present data and the experimental value of the thermal-neutron capture cross section [6], and the thin curves show its upper and lower limits with 1 standard deviation. The dashed curve and dash-dotted curve are the evaluated reaction rates with ENDF/B-VI [23] and JENDL-3.3 [15], respectively.

Using the obtained cross section for the ^{2}H$(n,\gamma)^3$H reaction, the Maxwellian-averaged neutron capture cross section for temperature T is given by

$$\frac{\langle\sigma v\rangle_{kT}}{v_T} = \frac{2}{\sqrt{\pi}}\frac{1}{(kT)^2} \times \int_0^\infty E_{\mathrm{c.m.}}\sigma_{^2\mathrm{H}}(n,\gamma: E_{\mathrm{c.m.}})\exp\left(\frac{-E_{\mathrm{c.m.}}}{kT}\right)dE_{\mathrm{c.m.}}, \quad (6)$$

where k is Boltzmann's constant, $v_T = (2kT/\mu)^{1/2}$ is the velocity corresponding to the thermal energy, kT, μ is the reduced mass in the entrance channel, and $E_{\mathrm{c.m.}}$ is the center-of-mass energy. Hence, the reaction rate is obtained with the uncertainty of about 8% as

$$N_A\langle\sigma v\rangle = 214 \times T_9^{0.075} + 742 \times T_9(\mathrm{cm}^3\,\mathrm{sec}^{-1}\,\mathrm{mole}^{-1}). \quad (7)$$

Here, T_9 is the temperature in units of 10^9 K and N_A is Avogadro's number. The uncertainty is the result of the combined uncertainties of the measured cross sections and the excitation curve obtained by fitting the measured cross sections. The reaction rate calculated by Fowler *et al.* [11] is

$$N_A\langle\sigma v\rangle = 66.2 + 1251 \times T_9(\mathrm{cm}^3\,\mathrm{sec}^{-1}\,\mathrm{mole}^{-1}). \quad (8)$$

The new reaction rate obtained in the present study is compared to that estimated assuming the charge symmetry while using the measured cross section of the ^{2}H$(p,\gamma)^3$He reaction [11], which now has large uncertainty as described above, in Fig. 6. The new rate differs also from the estimated value [11] and calculated values using evaluated cross sections in the ENDF/B-VI [23] and JENDL-3.3 [15]. It is quite large compared to the estimated value [11] for $T_9 < \sim 0.5$, and it is smaller for $T_9 > \sim 1$. Here, it should be noted that the evolution of primordial light element abundances in the bigbang occurs over the temperature range $T_9 \sim 0.1$–1 [28]. Therefore, it is necessary to quantitatively evaluate the primordial light element abundances in the standard big bang as well as in the nonstandard inhomogeneous big bang nucleosynthesis models using the new reaction rate. Especially, it would be quite interesting to see how the new rate would affect the ^{7}Li abundance, which is of current interest in the big-bang nucleosynthesis as described before. Note that the ^{2}H$(n,\gamma)^3$H reaction is one of the important reaction together with

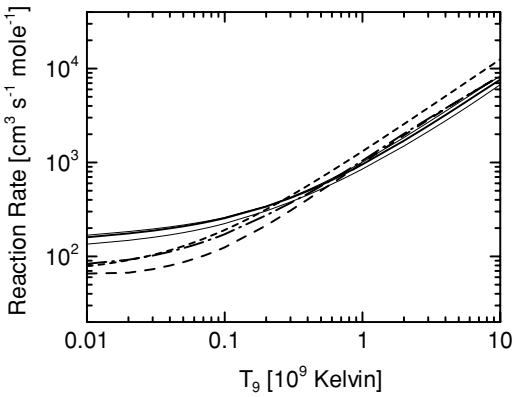

FIG. 6. Reaction rate vs the temperature in units of T_9. The thick solid curve is the reaction rate obtained in the present study, and the thin solid curves are its upper and lower limits with 1 standard deviation. The long-dashed curve is the reaction rate evaluated in FCZ67 [11]. The short-dashed and dash-dotted curves are the evaluated reaction rate with ENDF/B-VI [23] and JENDL-3.3 [15].

the ^{3}He$(n, p)^3$H and ^{2}H$(d, p)^3$H reactions to produce the primordial tritium, and the thus produced tritium is used to synthesize the primordial ^{7}Li via the ^{4}He$(t, \gamma)^7$Li reaction.

The reaction rate for the ^{2}H$(p, \gamma)^3$He reaction has been given as [3]

$$N_A\langle\sigma v\rangle = 1.71 \times 10^3 (T_9)^{-2/3} \exp\left[-\frac{3.72}{(T_9)^{1/3}}\right] \times [1 + 0.112(T_9)^{1/3} + 3.89(T_9)^{4/3}](\mathrm{cm}^3\,\mathrm{sec}^{-1}\,\mathrm{mole}^{-1}). \quad (9)$$

Because the charge symmetry is considered to hold well in the strong interaction, it is quite important to compare the new cross section for the ^{2}H$(n, \gamma)^3$H reaction to that for the ^{2}H$(p, \gamma)^3$He reaction, which is a key reaction during the proto-stars era as described before [2,3], and the accurate reaction cross section at low energy is highly required in the construction of models during the proto-stars. It is also worthwhile to use the present result to study the enhancement of the S factor due to the electron screening effects for the ^{2}H$(p, \gamma)^3$He reaction, which becomes significant at a low energy of around a few keV. Note that the new cross section differs from the previous one by a factor of $\sim$2.5 at $E_n \simeq$ 1 keV.

IV. SUMMARY

The ^{2}H$(n, \gamma)^3$H cross section has been measured in the neutron energy range from 10 to 80 keV and at $E_n =$ 531 keV by employing a discrete γ-ray detection method with the use of high sensitive anti-Compton NaI(Tl) spectrometers. The obtained cross sections differ significantly from the previously reported ones, but they are in good agreement with the calculated ones based on the Faddeev approach, which includes meson exchange currents as well as a three-body force. The new reaction rate differs from the values used so far, and therefore it would be quite interesting to study the consequences of the new rate on astrophysical applications.

ACKNOWLEDGMENTS

We thank T. Ohsaki for his useful discussion and K. Tosaka for his nice operation of the Pelletron accelerator. The experimental part of this work was supported by a grant-in-aid for scientific research of the Japan Ministry of Education, Culture, Sports, and Technology. The theoretical part of this work was supported by the Polish Committee for Scientific Research under grant 2P03B00825. The numerical calculations have been performed on the IBM Regatta p690+ of the NIC in Jülich, Germany.

[1] P. J. E. Peebles, Phys. Rev. Lett. **16**, 410 (1966); H. Sato, Prog. Theor. Phys. **38**, 1083 (1967); R. V. Wagoner, W. A. Fowler, and F. Hoyle, Astrophys. J. **148**, 3 (1967).
[2] S. W. Stahler, Astrophys. J. **332**, 804 (1988).
[3] C. Casella *et al.*, Nucl. Phys. **A706**, 203 (2002).
[4] J. H. Applegate, C. J. Hogan, and R. J. Scherrer, Phys. Rev. D **35**, 1151 (1987); R. A. Malaney and W. A. Fowler, Astrophys. J. **333**, 14 (1988).
[5] J. H. Applegate and C. J. Hogan, Phys. Rev. D **31**, 3037 (1985).
[6] L. Kaplan, G. R. Ringo, and K. E. Wilzbach, Phys. Rev. **87**, 785 (1952); V. P. Alfimenkov, S. B. Borzakov, É. V. Vasiléva, Vo Van Tkhuan, B. P. Osipenko, L. B. Pikelńer, V. G. Tishin, and É. I. Sharapov, Yad. Fiz. **32**, 1491 (1980) [Sov. J. Nucl. Phys. **32**, 771 (1980)]; E. T. Jurney, P. J. Bendt, and J. C. Browne, Phys. Rev. C **25**, 2810 (1982).
[7] A. E. Cox, S. A. R. Wynchank, and C. H. Collie, Nucl. Phys. **74**, 497 (1965).
[8] L. I. Schiff, Phys. Rev. **52**, 242 (1937); A. C. Philips, Nucl. Phys. **A184**, 337 (1972).
[9] J. L. Friar, B. F. Gibson, and G. L. Payne, Phys. Lett. **B251**, 11 (1990); J. Carlson, D. O. Riska, R. Schiavilla, and R. B. Wiringa, Phys. Rev. C **42**, 830 (1990).
[10] L. E. Marcucci, M. Viviani, R. Schiavilla, A. Kievsky, and S. Rosati, Phys. Rev. C **72**, 014001 (2005).
[11] W. A. Fowler, G. R. Caughlan, and B. A. Zimmerman, Annu. Rev. Astron. Astrophys. **5**, 525 (1967).
[12] G. J. Schmid, R. M. Chasteler, C. M. Laymon, H. R. Weller, R. M. Prior, and D. R. Tilley, Phys. Rev. C **52**, R1732 (1995); G. J. Schmid *et al.*, Phys. Rev. Lett. **76**, 3088 (1996).
[13] L. Ma, H. J. Karwowski, C. R. Brune, Z. Ayer, T. C. Black, J. C. Blackmon, E. J. Ludwig, M. Viviani, A. Kievsky, and R. Schiavilla, Phys. Rev. C **55**, 588 (1997).
[14] G. M. Griffiths, M. Lal, and C. D. Scarfe, Can. J. Phys. **41**, 724 (1963); G. M. Bailey, G. M. Griffiths, M. A. Olivo, and R. L. Helmer, Can. J. Phys. **48**, 3059 (1970).
[15] K. Shibata *et al.*, J. Nucl. Sci. Technol. **39**, 1125 (2002).

[16] ENDF/B-VI data file for ^{197}Au (MAT = 7925) 1993, evaluated by P. G. Young and E. D. Arthur.
[17] T. Ohsaki, Y. Nagai, M. Igashira, T. Shima, T. S. Suzuki, T. Kikuchi, T. Kobayashi, T. Takaoka, M. Kinoshita, and Y. Nobuhara, Nucl. Instrum. Methods A **425**, 302 (1999).
[18] M. Igashira, K. Tanaka, and K. Masuda, *Proceedings of the Conference of the 8th International Symposium on Capture Gamma-Ray and Related Topics* (World Scientific, Singapore, 1993), p. 992.
[19] C. A. Burke, M. T. Lunnon, and H. W. Lefevre, Phys. Rev. C **10**, 1299 (1974).
[20] Y. Nagai, T. S. Suzuki, T. Kikuchi, T. Shima, T. Kii, H. Sato, and M. Igashira, Phys. Rev. C **56**, 3173 (1997).
[21] M. Igashira, Y. Nagai, K. Masuda, T. Ohsaki, and H. Kitazawa, Astrophys. J. **441**, L89 (1995).
[22] K. Senoo, Y. Nagai, T. Shima, T. Ohsaki, and M. Igashira, Nucl. Instrum. Methods A **339**, 556 (1994).
[23] ENDF/B-VI data file for ^{2}H (MAT = 128) 1997, evaluated by P. G. Young, G. M. Hale, and M. B. Chadwick.
[24] J. Golak, R. Skibiński, H. Witała, W. Glöckle, A. Nogga, and H. Kamada, Phys. Rep. **415**, 89 (2005), and references therein.
[25] J. Golak, H. Kamada, H. Witała, W. Glöckle, J. Kuroś-Zołnierczuk, R. Skibiński, V. V. Kotlyar, K. Sagara, and H. Akiyoshi, Phys. Rev. C **62**, 054005 (2000).
[26] R. B. Wiringa, V. G. J. Stoks, and R. Schiavilla, Phys. Rev. C **51**, 38 (1995).
[27] B. S. Pudliner, V. R. Pandharipande, J. Carlson, S. C. Pieper, and R. B. Wiringa, Phys. Rev. C **56**, 1720 (1997).
[28] M. S. Smith, L. H. Kawano, and R. A. Malaney, Astrophys. J. Suppl. Ser. **85**, 219 (1993).